COMPDYN 2015
5th ECCOMAS Thematic Conference on
Computational Methods in Structural Dynamics and Earthquake Engineering
M. Papadrakakis, V. Papadopoulos, V. Plevris (eds.)
Crete Island, Greece, 25–27 May 2015

ENERGY METHOD FOR COUPLING NEWMARK AND α-SCHEMES TIME INTEGRATORS WITH DIFFERENT TIME STEPS

M. BRUN*, A. GRAVOUIL† AND A. COMBESCURE†

*Université de Lyon, INSA-Lyon, LGCIE, 34 rue des Arts, F-69621 Villeurbanne, France

†Université de Lyon, INSA-Lyon, LaMCoS, CNRS UMR5259, 18-20 rue des sciences, F-69621 Villeurbanne, France.
e-mail: michael.brun@insa-lyon.fr - Web page: ttp://lamcos.insa-lyon.fr/

Keywords: Structural dynamics, Heterogeneous Asynchronous time integrators, Hybrid multi-time methods, Energy conserving methods

Abstract. *The time integration procedure selected in computational structural dynamics must possess at least the stability and accuracy properties required for the convergence to the exact solution. Other desired properties are the unconditional stability for linear dynamics, second-order of accuracy, high frequency dissipation capabilities, self-starting, no overshoot, one step method and no more than one set of implicit equations to be solved for each time step (single-step-single-solve format). In linear dynamics, the stability is classically assessed by a spectral study of the amplification matrix, whereas physical energy bounds are preferred in nonlinear dynamics. Popular a-schemes (HHT-α, WBZ-α, CH-α) are second-order accurate and provides numerical dissipation for spurious high frequencies due to the finite element discretization. To go beyond the standard approach based on the same time integration scheme (homogeneous time integration scheme) and the same time step for all the finite elements of the mesh (synchronous time integration), the purpose of this paper is to describe a general methodology for building Heterogeneous (different time integration schemes such as Newmark or a-schemes) Asynchronous (different time steps) Time Integrators (HATI) for computational dynamics. The proposed HATI methods allow selecting the appropriate time integration scheme with its own time step in each part of the mesh following a dual Schur subdomain decomposition technique by introducing Lagrange multipliers for ensuring the velocity gluing at the subdomain interface. The key point for building the HATI methods is to cancel the interface pseudo-energy as introduced by Hughes in the so-called energy method employed for proving the stability of implicit-explicit algorithms in its pioneer works on heterogeneous time integrators. By canceling the pseudo-energy at the interface between subdomains and assuming a linear time variation of the Lagrange multipliers at the coarse time scale, two HATI methods are derived. The first new method, called BCG-macro method, for which the interface problem involving the Lagrange multipliers is solved at the large time scale, can handle any dissipative a-schemes (HHT-α, WBZ-α, CH-α), while preserving the second-order of accuracy when adopting different time steps. In addition to the energy argument (cancelation of the interface pseudo-energy), the stability and order of accuracy is proved by the spectral study of the amplification matrix. The*

second new method, called BGC-micro, is based on the velocity gluing at the fine time scale and can be viewed as an extension of the method proposed by Gravouil and Combescure (GC method) to the dissipative α-schemes.

1 INTRODUCTION

Partitioning approaches are very appealing with a view of coupling dynamic parts of a complex structure in a hybrid (experimental/numerical) real time testing. These hybrid tests require different explicit or implicit time integration schemes in different subdomains (called substructure in the context of hybrid testing) according to their complexity and characteristics. The purpose of such hybrid experimental/numerical testing such as the continuous pseudo-dynamic testing (PsD) is to test parts of the structure expected to experience some damage while the remainder of the whole structure is dealt numerically. As a consequence, the hybrid numerical-experimental testing techniques need to select high performance coupling methods from the field of computational mechanics in order to be able to make interact physical and numerical parts in real time (*Pinto et al.* [2004], *Brun et al.* [2012]). Typically, a reduced number of degrees of freedom is considered for the tested part but with a large number of small time steps: explicit time schemes are then adopted or other non-iterative time integration schemes (*Combescure and Pegon* [1997], *Bonnet et al.* [2008]).
In the numerical/experimental hybrid context, heterogeneous (different time schemes) asynchronous (different time steps) time integrators (HATI) have been investigated. Gravouil and Combescure proposed an HATI (*Gravouil and Combescure* [2001] and *Combescure and Gravouil* [2002]), called GC method, enabling explicit/implicit multi-time step computations on a partitioned domain: the non overlapping subdomains are coupled following on a dual approach, that is by prescribing the continuity of the velocity at the interface with the help of Lagrange multipliers. The stability of the GC method when considering any Newmark time integration schemes has been proven using the energy method, initially proposed by Hughes for deriving stability conditions for hybrid (implicit/explicit) time integrators. Beyond the widely used Newmark schemes, it is of great interest in structural dynamics to choose more advanced time integration schemes endowed with the following desirable properties: unconditional stability, second-order accuracy, no more than one set of implicit equations involved in the time step, self-starting, and controllable algorithmic dissipation in the higher modes. An excellent state of the art on the generalized single-step-single-solve (GSSSS) framework algorithms that encompasses the class of liner multi-time step methods (LMS) can be found in the works of Tamma and co-authors (*Masuri et al.* [2009c],*Masuri et al.* [2009a],*Masuri et al.* [2009b]).

In the context of the PsD tests, the staggered nature of the GC method (requiring in a first stage the computation of predictors followed by the solving of the interface problem finally completed with the correction of the predictors coming from the interface forces) clearly constitutes a drawback for carrying out experimental and numerical tasks in a concurrent way. Consequently, a new interfield parallel solution method, called the PM method from the authors' name (Pegon and Magonnette), has been described by Bonelli $et\ al.$ (*Bonelli et al.* [2008]) by coupling explicit and implicit time schemes. Recently, further efforts have been done to build coupling method able to handle the Generalized-α schemes proposed by Chung and Hulbert (*Chung and Hulbert* [1993]), well known for being able to control numerical damping and to filter out spurious high-frequency components of the response. The low-frequency are unaffected and the time integration scheme remains second-order accurate. Bursi $et\ al.$ (*Bursi et al.* [2010]) underline that the GC method based on the velocity continuity at the end time of the fine time steps is incompatible with the Generalized-α scheme whose terms involved into the equation of motion are weighted by different parameters. Therefore, in order to adapt the Generalized-α scheme to the end time collocation format of the GC coupling method, a new form of the Generalized-α scheme proposed by Arnold and Bruls (*Arnold and Bruls* [2007]) in

the multibody dynamic context is adopted, enforcing the equilibrium at the end of the time step instead of an averaged form as in the original time integrator. The derived interfield parallel solution method, called the PM-α method, is an extension to the α-schemes of the PM method (*Bursi et al.* [2010]).

Built upon the GC formulation, two other multi-time coupling schemes have been proposed. The first one is the PH method developed by Prakash and Hjelmstad (*Prakash and Hjelmstad* [2004]), assuming a velocity continuity at the macro-time scale (large time step) unlike the GC method based on the micro time scale (fine time step). It enables the dissipative drawback of the GC method to be tackled while optimizing the computation time related to the solving of the interface problem. The authors proved by using the energy-method that the pseudo-energy at the interface remains equal to zero. They concluded that the PH method is energy conserving when coupling non-dissipative Newmark schemes such as the implicit Constant Average Acceleration scheme (CAA) and the explicit Central Difference scheme (CD). Recently, the MGC method based on the macro time scale for the interface problem too, has been built with the focus of canceling the classical measure of the interface energy (*Mahjoubi et al.* [2011]). The derived method turns out to be able to couple Newmark schemes, HHT-α scheme (*Hilber et al.* [1977]), Simo scheme (*Simo and Tarnow* [1992]) and Krenk scheme (Balance Dissipation Scheme, *Krenk* [2008]) in linear dynamics. Nonetheless, the MGC coupling method uses a modified equation of motion for the HHT-α scheme: solving the equation of motion related to a given time step requires quantities one time step before, loosing the single solve single step format of the original HHT-α scheme.

In this paper, a general methodology based on energy considerations is described to obtain asynchronous coupling methods for different time integration schemes (Newmark, HHT-α, WBZ-α and CH-α)(*Brun et al.* [2015],**?**). The gluing of subdomains with their own time integrator and time step is ensured with Lagrange multipliers and velocity continuity. The key point for building stable HATI is to ensure the zero interface pseudo-energy, involved in the energy method for the DAE (Differential Algebraic Equation) stability analysis. On the other hand, the energy method argument is confirmed by carrying out a stability analysis performed from the amplification matrix linking state vectors at the beginning and at the end of the time step. Two new coupling methods, denoted in the following BGC-macro and BGC-micro methods, will be derived. The BGC-macro method is a macro-time-based method, such as the PH and MGC methods. It assumes a linear variation of the Lagrange multipliers over the macro-time step so as to lead to a kinematic condition at the interface, which, used together with the Lagrange multiplier variation assumption, guarantees the zero interface pseudo-energy. The method conserves the second order accuracy as highlighted by the convergence analysis. From the previous kinematic relationship, a second method is derived, called BGC-micro method, which handles the interface problem at the micro-time scale rather than at the macro time scale. Both proposed methods allow coupling α-schemes while conserving their original format, contrary to the MGC algorithm.

2 GENERAL METHODOLOGY FOR COUPLING α schemes

2.1 Unified format for the α-schemes

The time discretization is introduced as the following partition of the time domain: $t_0 < t_1 < \cdots < t_n < t_{n+1} < \cdots < t_f$ and h is the time step size assumed to be constant. Following the concept of weak equilibrium, the discretized equilibrium equation is only ensured at some times inside the time step. For the α-schemes, it corresponds to different weights applied to inertial, stiffness and external terms as given below (viscous terms are omitted in the following for the sake of simplicity):

$$\mathbf{M}\mathbf{a}_{n+\xi_m} + \mathbf{K}\mathbf{u}_{n+\xi_f} = \mathbf{f}_{n+\xi_f} - \mathbf{L}^T\boldsymbol{\lambda}_{n+\xi_f} \tag{1}$$

where $\mathbf{M}$, and $\mathbf{K}$, are the consistent mass matrix and the stiffness matrix. $\mathbf{L}$ is a linear kinematic constraint matrix at the boundary conditions. The discrete displacements, velocities and accelerations are designated by $\mathbf{u}$, $\mathbf{v}$ and $\mathbf{a}$. As external forces, the Lagrange multipliers required by the kinematic constraint is expressed at the time $t_{n+\xi_f}$. Using the two different averaged parameters ξ_m and ξ_f, the averaged displacements, velocities, accelerations and Lagrange multipliers read:

$$\begin{cases} \mathbf{a}_{n+\xi_m} = (1-\xi_m)\mathbf{a}_n + \xi_m\mathbf{a}_{n+1} \\ \mathbf{u}_{n+\xi_f} = (1-\xi_f)\mathbf{u}_n + \xi_f\mathbf{u}_{n+1} \\ \mathbf{f}_{ext,n+\xi_f} = (1-\xi_f)\mathbf{f}_{ext,n} + \xi_f\mathbf{f}_{ext,n+1} \\ \boldsymbol{\lambda}_{n+\xi_f} = (1-\xi_f)\boldsymbol{\lambda}_n + \xi_f\boldsymbol{\lambda}_{n+1} \end{cases} \tag{2}$$

The classical form for the Generalized-α scheme proposed by Chung and Hulbert (*Chung and Hulbert* [1993]) is characterized by two weighting parameters α_m and α_f. It writes:

$$\begin{aligned} (1-\alpha_m)\mathbf{M}\mathbf{a}_{n+1} + \alpha_m\mathbf{M}\mathbf{a}_n + (1-\alpha_f)\mathbf{K}\mathbf{u}_{n+1} + \alpha_f\mathbf{K}\mathbf{u}_{n+1} = \\ (1-\alpha_f)\mathbf{f}_{n+1} + (1-\alpha_f)\mathbf{f}_n - \mathbf{L}^T\boldsymbol{\lambda}_{n+1-\alpha_f} \end{aligned} \tag{3}$$

From the above averaged equilibrium equations in Eq. 1 and in Eq. 3, it can be easily seen that the following relationships between the algorithmic parameters hold: $\xi_m = 1 - \alpha_m$ and $\xi_f = 1 - \alpha_f$.

Optimized algorithmic parameters α_m, α_f, γ and β are given by the authors in order to achieve the unconditional stability, the second-order accuracy as well as the high-frequency dissipation while minimizing low-frequency dissipation. Three α-schemes are investigated : HHT-α (*Hilber et al.* [1977]), WBZ-α (*Wood et al.* [1981]) and CH-α (*Chung and Hulbert* [1993]). For all the three previous α-schemes, it is convenient to define the α_m and α_f parameters as a function of the the spectral radius at the high frequency limit (at infinity), noted as ρ_∞, characterizing the amount of dissipative energy in the high frequency range. The two other algorithmic parameters γ and β are involved in the classical Newmark formulae written below in terms of velocity increments:

$$\begin{cases} \Delta\mathbf{a} = \frac{1}{\gamma h}\Delta\mathbf{v} - \frac{1}{\gamma}\mathbf{a}_n \\ \Delta\mathbf{u} = \frac{\beta h}{\gamma}\Delta\mathbf{v} + h\mathbf{v}_n + \frac{\gamma-2\beta}{2\gamma}h^2\mathbf{a}_n \end{cases} \tag{4}$$

The algorithmic parameters γ and β are expressed in terms of α_m and α_f as it has been resumed in Table 1.

From Eq. 2, the averaged accelerations and displacements can be written as: $\mathbf{a}_{n+\xi_m} = \mathbf{a}_n +$

Scheme	α_m	α_f	γ	β
$HHT-\alpha$	0	$-\alpha_{HHT}=\frac{1-\rho_\infty}{1+\rho_\infty}$	$\frac{1}{2}-\alpha_{HHT}$	$\frac{1}{4}(1-\alpha_{HHT})^2$
$WBZ-\alpha$	$\alpha_{WBZ}=\frac{\rho_\infty-1}{1+\rho_\infty}$	0	$\frac{1}{2}-\alpha_{WBZ}$	$\frac{1}{4}(1-\alpha_{WBZ})^2$
$CH-\alpha$	$\frac{2\rho_\infty-1}{1+\rho_\infty}$	$\frac{\rho_\infty}{1+\rho_\infty}$	$\frac{3}{2}-2\alpha_f$	$(1-\alpha_f)^2$

Table 1: Relations between the spectral radius at infinity and the algorithmic parameters for the α-schemes enabling unconditional stability, second-order accuracy, optimized dissipative features.

$\xi_m\Delta\mathbf{a}$ and $\mathbf{u}_{n+\xi_f}=\mathbf{u}_n+\xi_f\Delta\mathbf{u}$. Incorporating theses expressions and the Newmark formulae in Eq. 4 into the equilibrium equation Eq. 1, we obtain a new format for the Generalized-α schemes as:

$$\mathbf{K}^*\Delta\mathbf{v}_{n+1}=\mathbf{g}_{n+1}-\mathbf{L}^T\boldsymbol{\lambda}_{n+\xi_f} \tag{5}$$

where the dynamic operator matrix is defined by $\mathbf{K}^*=\xi_m\frac{1}{\gamma h}\mathbf{M}+\xi_f\frac{\beta h}{\gamma}\mathbf{K}$. The right hand side vector $\mathbf{g}_{n+1}$ is expressed as:

$$\mathbf{g}_{n+1}=\mathbf{f}_{ext,n+\xi_f}-\mathbf{K}\mathbf{u}_n-\xi_f h\mathbf{K}\mathbf{v}_n+\xi_m\frac{1}{\gamma}M\mathbf{a}_n-M\mathbf{a}_n-\xi_f(\frac{\gamma-2\beta}{2\gamma})h^2\mathbf{K}\mathbf{a}_n \tag{6}$$

With a view to formulating the subdomain coupling algorithm, it is interesting to adopt a compact form for the complete-three stage time-stepping of the α-schemes as:

$$\mathbb{K}^*\Delta\mathbb{U}_{n+1}+\mathbb{L}^T\boldsymbol{\lambda}_{n+\xi_f}=\mathbb{G}_{n+1} \tag{7}$$

The vector $\Delta\mathbb{U}_{n+1}$ gathers the increments of velocities, displacements and accelerations: $\Delta\mathbb{U}_{n+1}^T=\left[\begin{array}{ccc}\Delta\mathbf{v} & \Delta\mathbf{u} & \Delta\mathbf{a}\end{array}\right]$. $\mathbb{L}$ is the constraint matrix: $\mathbb{L}=\left[\begin{array}{ccc}\mathbf{L} & \mathbf{0} & \mathbf{0}\end{array}\right]$. The right hand side vector is given by:

$$\mathbb{G}_{n+1}=\mathbb{F}_{n+\xi_f}-\mathbb{N}\mathbb{U}_n \tag{8}$$

where $\mathbb{F}_{n+\xi_f}^T=\left[\begin{array}{ccc}\mathbf{f}_{ext,n+\xi_f} & \mathbf{0} & \mathbf{0}\end{array}\right]$. The expressions of the matrix $\mathbb{K}^*$ and the matrix $\mathbb{N}$ are:

$$\mathbb{K}^*=\left[\begin{array}{ccc}\mathbf{K}^* & \mathbf{0} & \mathbf{0}\\ -\frac{\beta h}{\gamma}\mathbf{I} & \mathbf{I} & \mathbf{0}\\ -\frac{1}{\gamma h}\mathbf{I} & \mathbf{0} & \mathbf{I}\end{array}\right],\mathbb{N}=\left[\begin{array}{ccc}\xi_f h\mathbf{K} & \mathbf{K} & \xi_f\left(\frac{\gamma-2\beta}{2\gamma}\right)h^2\mathbf{K}+\left(1-\xi_m\frac{1}{\gamma}\right)\mathbf{M}\\ h\mathbf{I} & \mathbf{0} & \left(\frac{\gamma-2\beta}{2\gamma}\right)h^2\mathbf{I}\\ \mathbf{0} & \mathbf{0} & -\frac{1}{\gamma}\mathbf{I}\end{array}\right] \tag{9}$$

2.2 Coupling with heterogeneous time steps

In order to formulate the coupling between two subdomains, we employ the previous unified form of the equilibrium equations at t_{γ_A} for the subdomain Ω_A (macro time scale), and at a series of times $t_{j-1+\gamma_B}$ for the subdomain Ω_B (micro time scale); first, for the macro subdomain Ω_A:

$$\left\{\begin{array}{l}\mathbf{K}_A^*\Delta\mathbf{v}_m^A+\mathbf{L}_A^T\boldsymbol{\lambda}_{\xi_{A,f}}=\mathbf{g}_m^A\\ \Delta\mathbf{u}_m^A=\frac{\beta_A h_A}{\gamma_A}\Delta\mathbf{v}_m^A+h_A\mathbf{v}_0^A+\frac{\gamma_A-2\beta_A}{2\gamma_A}h_A^2\mathbf{a}_0\\ \Delta\mathbf{a}_m^A=\frac{1}{\gamma_A h_A}\Delta\mathbf{v}_m^A-\frac{1}{\gamma_A}\mathbf{a}_0^A\end{array}\right. \tag{10}$$

Secondly, for the micro subdomain Ω_B:

$$\begin{cases} \mathbf{K}_B^* \Delta \mathbf{v}_j^B + \mathbf{L}_B^T \boldsymbol{\lambda}_{j-1+\xi_{B,f}} = \mathbf{g}_j^B \\ \Delta \mathbf{u}_j^B = \frac{\beta_B h_B}{\gamma_B} \Delta \mathbf{v}_j^B + h_B \mathbf{v}_{j-1}^B + \frac{\gamma_B - 2\beta_B}{2\gamma_B} h_B^2 \mathbf{a}_{j-1} \\ \Delta \mathbf{a}_j^B = \frac{1}{\gamma_B h_B} \Delta \mathbf{v}_j^B - \frac{1}{\gamma_B} \mathbf{a}_{j-1}^B \\ \forall j \in \{1, m\} \end{cases} \tag{11}$$

The above equations can also be given in a compact form as:

$$\mathbb{K}_{\mathbb{A}}^* \Delta \mathbb{U}_m^A + \mathbb{L}_A^T \boldsymbol{\lambda}_{\xi_{A,f}} = \mathbb{F}_{\xi_{A,f}}^A - \mathbb{N}_A \mathbb{U}_0^A \tag{12}$$

and

$$\mathbb{K}_{\mathbb{B}}^* \Delta \mathbb{U}_j^A + \mathbb{L}_B^T \boldsymbol{\lambda}_{j-1+\xi_{B,f}} = \mathbb{F}_{j-1+\xi_{B,f}}^B - \mathbb{N}_B \mathbb{U}_{j-1}^B \; \forall j \in \{1, m\} \tag{13}$$

The kinematic equation at the interface will complete the system of equations for coupling the two subdomains with heterogeneous time steps. It will be shown in the following that ensuring the zero energy at the interface in terms of the pseudo-energy norm as introduced by Hughes in the energy method (*Hughes* [1987]), enables a kinematic condition for velocity increments to be derived.

3 BGC-MACRO METHOD FROM THE ENERGY METHOD

The energy method proposed by Hughes has been widely used for obtaining the stability conditions for coupling schemes, mixing implicit and explicit schemes (*Hughes* [1987]). For example, the stability of the GC method and the PH method has been proven by this way (*Combescure and Gravouil* [2002], *Prakash and Hjelmstad* [2004]). It consists in proving that the interface pseudo-energy is equal or less than zero. Here, the interface pseudo-energy is employed as the starting point of the new coupling methods by ensuring the zero interface pseudo-energy. Thus, the following coupling schemes are built from the discrete balance equation given in the energy method in terms of pseudo-energy. For a given subdomain (by omitting the scripts for belonging subdomains), the pseudo-energy balance equation is given by:

$$\left[\frac{1}{2} \mathbf{a}^T \mathbf{A} \mathbf{a} + \frac{1}{2} \mathbf{v}^T \mathbf{K} \mathbf{v} \right]_n^{n+1} = \frac{1}{h} \Delta \mathbf{v}^T \left\{ (\mathbf{f}_{ext,n+1} - \mathbf{f}_{ext,n}) \right\} - (\gamma - \frac{1}{2}) \left\{ \Delta \mathbf{a}^T \mathbf{A} \Delta \mathbf{a} \right\} \tag{14}$$

in which the matrix $\mathbf{A}$ is defined by $\mathbf{A} = \mathbf{M} + \left(\beta - \frac{1}{2}\gamma\right) h^2 \mathbf{K}$. The previous balance equation can also be noted as:

$$\Delta E_{kin} + \Delta E_{int} = \Delta E_{ext} + \Delta E_{diss} \tag{15}$$

where ΔE_{kin}, ΔE_{int}, ΔE_{ext} and ΔE_{diss} are the increments over the time step of pseudo-energies which can be related to the classical kinetic, internal, external and dissipated energies.

Considering two subdomains Ω_A and Ω_B, the global discrete pseudo-energy balance equation takes into account the above contributions from both subdomains on the macro time step $h_A = [t_0; t_m]$ and on the series of the micro time steps $h_B = [t_{j-1}; t_j]$ for j varying from 1 to m, plus an additional term corresponding to the interface energy. The discrete pseudo-energy balance

equation over the macro time step $h_A = [t_0; t_m]$ for the whole domain is given below:

$$\Delta E^A_{kin,m} + \Delta E^A_{int,m} + \sum_{j=1}^{m} \left\{ \Delta E^B_{kin,j} + \Delta E^B_{int,j} \right\} = \dots$$

$$\Delta E^A_{ext,m} + \sum_{j=1}^{m} \Delta E^B_{ext,j} + \Delta E^A_{diss,m} + \sum_{j=1}^{m} \Delta E^B_{diss,j} + \Delta E_{interface} \tag{16}$$

The interface pseudo-energy (*Prakash and Hjelmstad* [2004]) can be written as:

$$\Delta E_{interface} = -\frac{1}{h_A} \Delta \mathbf{v_m^A}^T \left\{ \mathbf{L}_A^T \left(\boldsymbol{\lambda}_m - \boldsymbol{\lambda}_0 \right) \right\} - \sum_{j=1}^{m} \left\{ \frac{1}{h_B} \Delta \mathbf{v_j^B}^T \left\{ \mathbf{L}_B^T \left(\boldsymbol{\lambda}_j - \boldsymbol{\lambda}_{j-1} \right) \right\} \right\} \tag{17}$$

The pseudo-energy method has to be distinguished from the discretized energy balance equation (*Hughes* [1987] and *Brun et al.* [2014]). The pseudo-energy is dedicated to stability analysis whereas the classical energy balance equation enables to build energy-preserving time integrators. It has to be noted that the above equation can be seen as a generalization of the pseudo-energy method related to the study of ODE (Ordinary Differential Equation) stability to the study of DAE (Differential Algebraic Equation) stability, that is with Lagrange multipliers. This stability method based on the energetic view point will be confirmed in the last section by a classical amplification matrix spectral analysis, with state vectors gathering kinematic quantities and Lagrange multipliers. The coupling method is considered to be stable if the total pseudo-energy variation (kinetic plus internal pseudo-energy variations) over the macro time step under zero external loads is less than or equal to zero. Consequently, it is sufficient to prove that the pseudo-energy at the interface $E_{interface}$ is less than or equal to zero. It has to be reminded that the energy conservative features of the PH method (*Prakash and Hjelmstad* [2004]) has been demonstrated $a\ posteriori$. In contrast to the PH method , the coupling method here enables to satisfy the energy conservative feature $a\ priori$ by ensuring the zero interface pseudo-energy over the macro time step. For this purpose, an assumption related to the time variation of the Lagrange multipliers over the macro time step is required: we assume that the Lagrange multipliers at the micro scale can be linearly interpolated from the Lagrange multipliers given at the beginning and the end of macro time step. So we have:

$$\boldsymbol{\lambda}_j - \boldsymbol{\lambda}_{j-1} = \frac{\boldsymbol{\lambda}_m - \boldsymbol{\lambda}_0}{m} \tag{18}$$

Consequently, the interface pseudo-energy can be simplified as:

$$\Delta E_{interface} = -\left[\frac{1}{h_A} \Delta \mathbf{v}_m^{A\,T} \mathbf{L}_A^T + \sum_{j=1}^{m} \left\{ \frac{1}{m h_B} \Delta \mathbf{v}_j^{B\,T} \mathbf{L}_B^T \right\} \right] \left(\boldsymbol{\lambda}_m - \boldsymbol{\lambda}_0 \right) \tag{19}$$

Finally, the zero interface pseudo-energy requirement leads to the following kinematic equation:

$$\mathbf{L}_A \Delta \mathbf{v}_m^A + \sum_{j=1}^{m} \mathbf{L}_B \Delta \mathbf{v}_j^B = 0 \tag{20}$$

Considering two subdomains Ω_A and Ω_B with different time scales, m being equal to the time step ratio, the interface forces associated with the subdomain Ω_A are computed at the

time $t_{\xi_{A,f}} = \xi_{A,f} t_0 + (1-\xi_{A,f}) t_m$ belonging to the macro-time step $h_A = [t_0; t_m]$, whereas the interface forces associated with the subdomain Ω_B are computed at the time $t_{j-1+\xi_{B,f}} = \xi_{B,f} t_{j-1} + (1-\xi_{B,f}) t_j$ belonging to the micro-time step $h_B = [t_{j-1}; t_j]$ for j varying from 1 to m. By using the linear relationship for Lagrange multipliers, we can write the interface forces for both subdomains as:

$$\left\{ \begin{array}{l} \mathbf{L}_A^T \boldsymbol{\lambda}_{\xi_{A,f}} = \mathbf{E}_{A,m}^T \boldsymbol{\lambda}_0 + \mathbf{C}_{A,m}^T \boldsymbol{\lambda}_m \\ \mathbf{L}_B^T \boldsymbol{\lambda}_{j-1+\xi_{B,f}} = \mathbf{E}_{B,j}^T \boldsymbol{\lambda}_{j-1} + \mathbf{C}_{B,j}^T \boldsymbol{\lambda}_j \end{array} \right. \tag{21}$$

with:

$$\left\{ \begin{array}{l} \mathbf{E}_{A,m}^T = (1-\xi_{A,f}) \mathbf{L}_A^T \\ \mathbf{C}_{A,m}^T = \xi_{A,f} \mathbf{L}_A^T \\ \mathbf{E}_{B,j}^T = \left[(1-\xi_{B,f})(1-\frac{j-1}{m}) + \xi_{B,f}(1-\frac{j}{m}) \right] \mathbf{L}_B^T \\ \mathbf{C}_{B,j}^T = \left[(1-\xi_{B,f})(\frac{j-1}{m}) + \xi_{B,f}(\frac{j}{m}) \right] \mathbf{L}_B^T \quad \forall j \in [1,m] \end{array} \right. \tag{22}$$

Then, the global system of equilibrium equations is obtained by gathering the compact forms of the three-stage time stepping schemes for both subdomains. It writes:

$$\left[\begin{array}{ccccc|c|c} \mathbb{K}_B^* & & & & & & \mathbb{C}_{B,1}^T \\ \mathbb{N}_B & \mathbb{K}_B^* & & & & & \mathbb{C}_{B,2}^T \\ \mathbb{N}_B & \mathbb{N}_B & \mathbb{K}_B^* & & & & \mathbb{C}_{B,3}^T \\ & \ddots & \ddots & \ddots & & & \vdots \\ \mathbb{N}_B & \mathbb{N}_B & \mathbb{N}_B & \mathbb{N}_B & \mathbb{K}_B^* & & \mathbb{C}_{B,m}^T \\ \hline & & & & & \mathbb{K}_A^* & \mathbb{C}_{A,m}^T \\ \hline \mathbb{L}_B & \mathbb{L}_B & \mathbb{L}_B & \cdots & \mathbb{L}_B & \mathbb{L}_A & \mathbf{0} \end{array} \right] \left[\begin{array}{c} \Delta \mathbb{U}_1^B \\ \Delta \mathbb{U}_2^B \\ \Delta \mathbb{U}_3^B \\ \vdots \\ \Delta \mathbb{U}_m^B \\ \hline \Delta \mathbb{U}_m^A \\ \hline \boldsymbol{\lambda}_m \end{array} \right] = \left[\begin{array}{c} \mathbb{F}_{\xi_{B,f}}^B - \mathbb{N}_B \mathbb{U}_0^B - \mathbb{E}_{B,1}^T \boldsymbol{\lambda}_0 \\ \mathbb{F}_{1+\xi_{B,f}}^B - \mathbb{N}_B \mathbb{U}_0^B - \mathbb{E}_{B,2}^T \boldsymbol{\lambda}_0 \\ \mathbb{F}_{2+\xi_{B,f}}^B - \mathbb{N}_B \mathbb{U}_0^B - \mathbb{E}_{B,3}^T \boldsymbol{\lambda}_0 \\ \vdots \\ \mathbb{F}_{m-1+\xi_{B,f}}^B - \mathbb{N}_B \mathbb{U}_0^B - \mathbb{E}_{B,m}^T \boldsymbol{\lambda}_0 \\ \hline \mathbb{F}_{\xi_{A,f}}^A - \mathbb{N}_A \mathbb{U}_0^A - \mathbb{E}_{A,m}^T \boldsymbol{\lambda}_0 \\ \hline \mathbf{0} \end{array} \right] \tag{23}$$

4 BGC-MICRO METHOD FROM THE ENERGY METHOD

From the kinematic relationship at the macro time step in Eq. 20, it is easy to define a similar relationship at the micro time step as:

$$\frac{1}{m} \mathbf{L}_A \Delta \mathbf{v}_m^A + \mathbf{L}_B \Delta \mathbf{v}_j^B = 0 \ \ \forall j \in [1,m] \tag{24}$$

The Lagrange multipliers are computed at the times $t_0 + \xi_{A_f}$ and $t_{j-1} + \xi_{B_f}$ for the subdomains Ω_A and Ω_B as:

$$\left\{ \begin{array}{l} \boldsymbol{\lambda}_{\xi_{A,f}} = \boldsymbol{\lambda}_0 + \xi_{A,f} \sum_{k=1}^m \Delta \boldsymbol{\lambda}_k \\ \boldsymbol{\lambda}_{j-1+\xi_{B,f}} = \boldsymbol{\lambda}_{j-1} + \xi_{B,f} \Delta \boldsymbol{\lambda}_j \end{array} \right. \tag{25}$$

Assuming the increment of the Lagrange multipliers $\Delta \boldsymbol{\lambda}_k$ is constant over the macro time step h_A, the interface equation at the micro time step can be rewritten for the α-schemes as (*Brun et al.* [2015]):

$$\mathbf{H} \Delta \boldsymbol{\lambda}_j = \mathbf{b}_j \tag{26}$$

in which the interface operator at the micro time scale and the right hand side vector are defined by:

$$\begin{cases} \mathbf{H} = \left[\xi_{A,f}\mathbf{L}_A(\mathbf{K}_A^*)^{-1}\mathbf{L}_A^T + \xi_{B,f}\mathbf{L}_B(\mathbf{K}_B^*)^{-1}\mathbf{L}_B^T\right] \\ \mathbf{b}_j = \frac{1}{m}\mathbf{L}_A\Delta\mathbf{v}_{free,m}^A + L_B\Delta\mathbf{v}_{free,j}^B - \frac{1}{m}\mathbf{L}_A(\mathbf{K}_A^*)^{-1}\mathbf{L}_A^T\boldsymbol{\lambda}_0 - \mathbf{L}_B(\mathbf{K}_B^*)^{-1}\mathbf{L}_B^T\boldsymbol{\lambda}_{j-1} \end{cases} \tag{27}$$

5 CONVERGENCE ANALYSIS

The BGC-macro method preserves exactly the pseudo-interface energy, proving the stability of the coupling algorithm. It remains to analyse the accuracy order of the coupling algorithm. Along the lines of *Bonelli et al.* [2008] and *Bursi et al.* [2010], an alternative convergence analysis is investigated by the spectral analysis of the amplification matrix $\mathbf{A}$, linking a state vector at the time $t_n + h_A = t_{n+1}$ to the previous state vector t_n. In addition to the stability, the amplification matrix enables to derive the accuracy order as well as the algorithmic damping ratio and the period elongation error related to the coupling algorithm. The convergence of the BGC-macro method is carried out for a single degree of freedom system, split into two subdomains Ω_A and Ω_B. The BGC-macro method is recast into the following recursive form:

$$\mathbf{X}_{n+1} = \mathbf{A}\mathbf{X}_n + \mathbf{L}_n \tag{28}$$

where $\mathbf{X}$ is an appropriate state vector depending on the formulation of the time integration algorithm, $\mathbf{A}$ is the amplification matrix and $\mathbf{L}$ is the load vector depending on the external forces. The BGC-macro method adopts the following state vector at time t_n:

$$\mathbf{X}_n = \left[\mathbf{X}_n^A \;\; \mathbf{X}_n^B\right]^T \tag{29}$$

where $\mathbf{X}_n^A$, $\mathbf{X}_n^B$ are the state vectors related the subdomains Ω_A and Ω_B, respectively. $\mathbf{X}_n^A$ collects the kinematic quantities of subdomain Ω_A, including the Lagrange multiplier at the macro time scale:

$$\mathbf{X}_n^A = \left[\mathbf{u}_n^A \;\; \mathbf{v}_n^A \;\; \mathbf{a}_n^A \;\; \boldsymbol{\lambda}_n\right]^T \tag{30}$$

It is important to remark that the state vector includes the Lagrange multiplier contrary to the PM method proposed by Bonelli $et\ al$ *Bonelli et al.* [2008] and Bursi $et\ al$ *Bursi et al.* [2010], including instead the free velocity related to the subdomain Ω_A.
$\mathbf{X}_n^B$ collects the kinematic quantities of subdomain Ω_B:

$$\mathbf{X}_n^B = \left[\mathbf{u}_n^B \;\; \mathbf{v}_n^B \;\; \mathbf{a}_n^B\right]^T \tag{31}$$

For the split oscillator, the state vector $\mathbf{X}_n$ gathers 7 components. In the following, we do not consider the load vector $\mathbf{L}_n$ because we assume that the leading error term of its approximation is greater than the order of accuracy of the method. It has been in *Brun et al.* [2014] that Eq. 28 can be developed as:

$$\begin{bmatrix} \mathbf{X}_{n+1}^A \\ \mathbf{X}_{n+1}^B \end{bmatrix} = \begin{bmatrix} \mathbf{A}^{AA} & \mathbf{A}^{AB} \\ \mathbf{A}^{BA} & \mathbf{A}^{BB} \end{bmatrix} \begin{bmatrix} \mathbf{X}_n^A \\ \mathbf{X}_n^B \end{bmatrix} \tag{32}$$

where the matrices $\mathbf{A}^{AA}$, $\mathbf{A}^{AB}$, $\mathbf{A}^{BA}$ and $\mathbf{A}^{BB}$ depend on the time step ratio, noted in the following as ss. The split oscillator is defined by the following mass and stiffness decomposition: $m = m^A + m^B$, $k = k^A + k^B$ with the ratio $b_1 = \frac{m^A}{m^B} = \frac{k^B}{k^A}$. The amplification matrix is

too complex for a closed-form expression as soon as different time steps are used. As a consequence, the amplification matrix is numerically computed for different values of time integrator parameters (ρ_∞ for CH-α schemes), mass and stiffness ratio b_1 and time step ratio ss. To address the accuracy, an alternative form of the amplification matrix is considered (*Bonelli et al.* [2008], *Bursi et al.* [2010]):

$$\bar{\mathbf{A}} = \bar{\mathbf{M}}\mathbf{A}\bar{\mathbf{M}}^{-1} \tag{33}$$

with the state vector modified as:

$$\bar{\mathbf{X}}_n = \left[\mathbf{u}_n^A \;\; \mathbf{v}_n^A \;\; h_A\mathbf{a}_n^A \;\; h_A\boldsymbol{\lambda}_n \;\; \mathbf{u}_n^B \;\; \mathbf{v}_n^B \;\; h_A\mathbf{a}_n^B\right]^T \tag{34}$$

and the matrix $\bar{\mathbf{M}}$ given by:

$$\bar{\mathbf{M}} = block\ diagonal\left[\mathbf{I} \;\; \mathbf{I} \;\; h_A\mathbf{I} \;\; h_A\mathbf{I} \;\; \mathbf{I} \;\; \mathbf{I} \;\; h_A\mathbf{I}\right]^T \tag{35}$$

where $\mathbf{I}$ is the identity matrix (equal to 1 in the case of the split oscillator).

Let us begin with the study of the stability of the BGC-macro method. The absolute stability of the BGC-macro method is investigated by computing the seven eigenvalues of the amplification matrix $\mathbf{A}$ in the case of the split-oscillator. The eigenvectors are linearly independent for each repeated eigenvalues λ_i. Hence, the condition $|\lambda_i| \leq 1$, for $i = 1...7$, is sufficient to demonstrate the A-stability of the method. In Figure 1, the coupling between two CH-α schemes (spectral radii $\rho_\infty = 0.8$ and $\rho_\infty = 0.5$ for the two subdomains at the coarse and fine time scales, respectively) is investigated as a function of the time step ratio ss by plotting the absolute values of the eigenvalues as a function of the reduced angular frequency $\Omega_B = \omega_B h_B$. Among the seven eigenvalues, only one pair is complex conjugate, giving the principal eigenvalues, whereas the five remaining are the spurious ones. In all investigated cases (any ρ_∞ and b_1), the BGC-macro method is found to be unconditionally stable when coupling unconditionally stable time integrators.

The local truncation error $\bar{\tau}_n$ is defined as

$$\bar{\tau}_n = \bar{\mathbf{A}}\bar{\mathbf{X}}(t_n) - \bar{\mathbf{X}}(t_{n+1}) \tag{36}$$

where $\bar{\mathbf{X}}(t_n)$ and $\bar{\mathbf{X}}(t_{n+1})$ correspond to the exact solutions of the state vector at the time t_n and t_{n+1}. From numerical calculations, the order of the truncation error can be assessed by computing the slope of $\ln(\bar{\tau}_n)$ as a function of the macro time step h_A. Indeed, the power k of the leading term of the local truncation error $\bar{\tau}_n = \alpha h_A^k + O(h_A^{k+1})$ (α being a constant) can be computed as: $k = \frac{\ln(\bar{\tau}_n(h_{2,A})) - \ln(\bar{\tau}_n(h_{1,A}))}{\ln(h_{2,A}) - \ln(h_{1,A})}$, where $\bar{\tau}_n(h_{2,A})$ and $\bar{\tau}_n(h_{1,A})$ are the numerical results of the local truncation error for two different small values of the macro time step h_A, with $h_{1,A} < h_{2,A}$. One obtains

$$\bar{\tau}_n = O(h_A^3) \tag{37}$$

for any values of the time step ratio ss. It is worth noting that the same result has been obtained in *Bonelli et al.* [2008] (Newmark schemes) and *Bursi et al.* [2010] (α-schemes) for the PM method, but only in the case of the same time step in both subdomains. Indeed, as soon as different time steps are adopted, the PM method only exhibits $\bar{\tau}_n = O(h_A^2)$.

For illustration, the local truncation error is plotted in Figure 2 for a time step ratio $ss = 2$. It can be seen that the power k of the leading term of the local truncation error depends on the quantity under consideration (displacement, velocity, acceleration and Lagrange multiplier). In details, we have: $\bar{\tau}_u^A = O(h_A^4)$, $\bar{\tau}_v^A = O(h_A^3)$, $\bar{\tau}_a^A = O(h_A^3)$, $\bar{\tau}_\lambda^A = O(h_A^3)$, $\bar{\tau}_u^B = O(h_A^4)$, $\bar{\tau}_v^B = O(h_A^3)$, $\bar{\tau}_a^B = O(h_A^3)$.

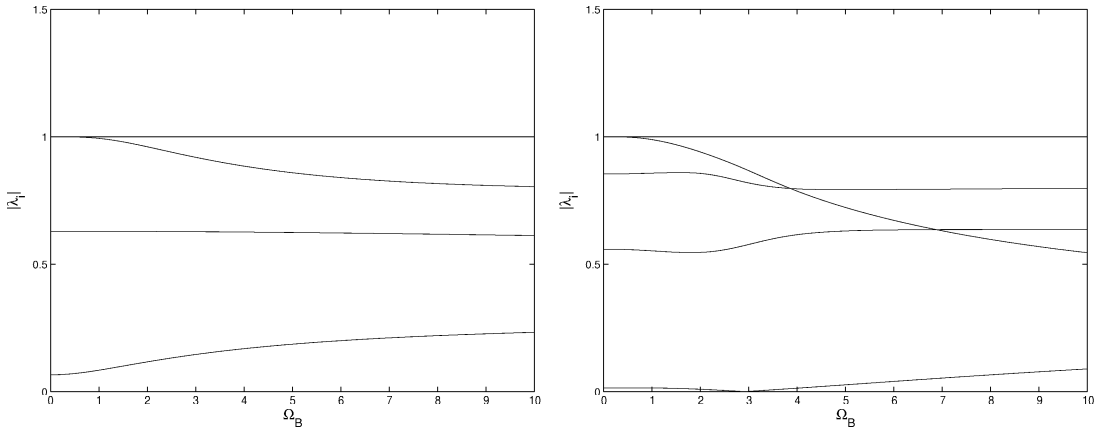

(a) ss=1 (b) ss=2

(c) ss=5 (d) ss=10

Figure 1: $|\lambda_i|$ of the split oscillator ($b_1 = 1$) for the BGC-macro method: CH-α ($\rho_\infty = 0.8$) coupled with CH-α ($\rho_\infty = 0.5$) with different time step ratios ss.

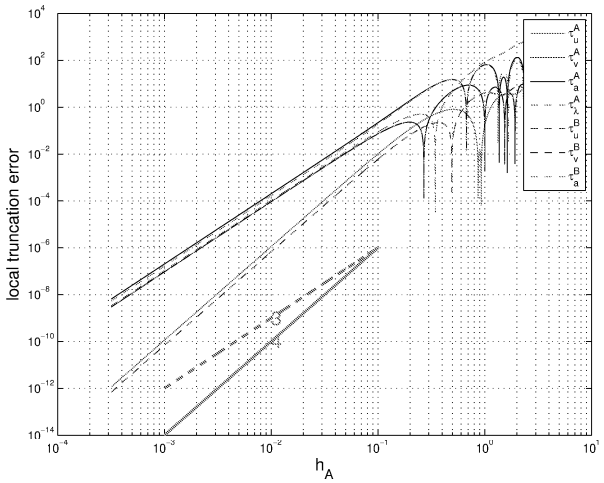

Figure 2: Local truncation error $\bar{\tau}$ of the split oscillator ($b_1 = 1$): CH-α ($\rho_\infty = 0.8$) coupled with CH-α ($\rho_\infty = 0.5$) with time step ratios $ss = 2$.

According to the Lax equivalence theorem (following the arguments of *Bonelli et al.* [2008] and *Bursi et al.* [2010]), a method will be convergent of the order k, if it is stable and consistent of the order k, $i.e.$ $\bar{\tau}_n = O(h_A^{k+1})$. As a result, the BGC-macro method is convergent of the order 2 for any time step ratio.
It is important to underline that the second order accuracy of the α-schemes is preserved through coupling with the BGC-macro method, which is not the case for the algorithms proposed in the literature (*Bursi et al.* [2010]). The last point of this convergence analysis concerns the numerical damping ratio and the relative period error. We define the nondimensional frequency of the whole system as $\Omega = \omega h_A$. The principal complex conjugate eigenvalues of the amplification matrix can be expressed as (*Bonelli et al.* [2008],*Geradin and Rixen* [1993]):

$$\lambda_{1,2} = e^{-\bar{\xi}\bar{\omega}h_A \pm i\bar{\omega}h_A} \tag{38}$$

where $\bar{\xi}$ is the numerical damping ratio and $\bar{\omega}$ the numerical angular frequency. In Figure 3, the numerical damping ratio related to BGC-macro method for a time step ratio ss equal to 1 is compared with numerical damping ratio for a time step ratio higher than 1 when coupling CH-α schemes with $\rho_\infty = 0.8$ and $\rho_\infty = 0.5$ for the two subdomains (coarse and fine time scales). It can be checked that the slope at small values of Ω seems not to be altered by the multi-time step algorithm. More precisely, the order of the damping ratio is assessed by computing $\frac{\ln(\bar{\xi}(h_{2,A}))-\ln(\bar{\xi}(h_{1,A}))}{\ln(h_{2,A})-\ln(h_{1,A})}$ where $h_{1,A}$ and $h_{2,A}$ are small values of macro time step. It enables to conclude about the order of the leading low-frequency damping term. One obtains: $\bar{\xi} = O(\Omega^3)$ for any time step ratio ss. It can be verified that this order of accuracy corresponds to the leading low-frequency term of the α-schemes without coupling (*Krenk* [2008], *Krenk and Hogsberg* [2005]). It is also important to highlight that there is a marked difference between classical GC algorithm and the proposed BGC-macro algorithm in the case of Newmark schemes. By carrying out the same analysis for the GC method, along the lines of Bonelli $et\ al$ (*Bonelli et al.* [2008]) conducted for their PM method, the damping ratio obtained for the GC method is compared to the one for the BGC-macro method for two implicit CAA Newmark schemes in Figure 3. It can be seen that the order of the leading term in the damping ratio is equal to 1 for the GC algorithm ($\bar{\xi} = O(\Omega)$) whereas the BGC-macro method maintains the zero damping values of the CAA schemes.

Last, the numerical elongation period is studied. It is defined as $\frac{\bar{T}-T}{T}$, where $\bar{T} = \frac{2\pi}{\bar{\omega}}$. In Figure 4, period elongations for different time step ratios ss are compared when considering CH-α schemes ($\rho_\infty = 0.8$ and $\rho_\infty = 0.5$ for the two subdomains). Again, the leading low-frequency term in the period elongation is assessed and one obtains $\frac{\bar{T}-T}{T} = O(\Omega^2)$, corresponding to the classical result for α-schemes (*Krenk and Hogsberg* [2005], *Geradin and Rixen* [1993]). When coupling CAA schemes, the BGC-macro method generates a very similar period elongation to the one generated by the GC method. The leading low-frequency term is equal to 2, corresponding to the classical result for the Newmark schemes (*Geradin and Rixen* [1993]). Thus, the GC coupling alters the leading low-frequency damping term but not the period elongation one.
To resume, the BGC-macro method provides $\xi = O(\Omega^3)$ and $\frac{\bar{T}-T}{T} = O(\Omega^2)$ for the α-schemes and for any time step ratios ss, as offered by the α scheme without coupling, confirming the second order of accuracy. For CAA schemes, the BGC-macro method provides $\bar{\xi} = 0$ and $\frac{\bar{T}-T}{T} = O(\Omega^2)$ for any time step ratios ss, as offered by the CAA scheme without coupling, confirming the second order of accuracy.
In conclusion, the stability, second order accuracy and convergence of the α-schemes are preserved through coupling with the BGC-macro method thanks to its conservation law based on the interface pseudo-energy.

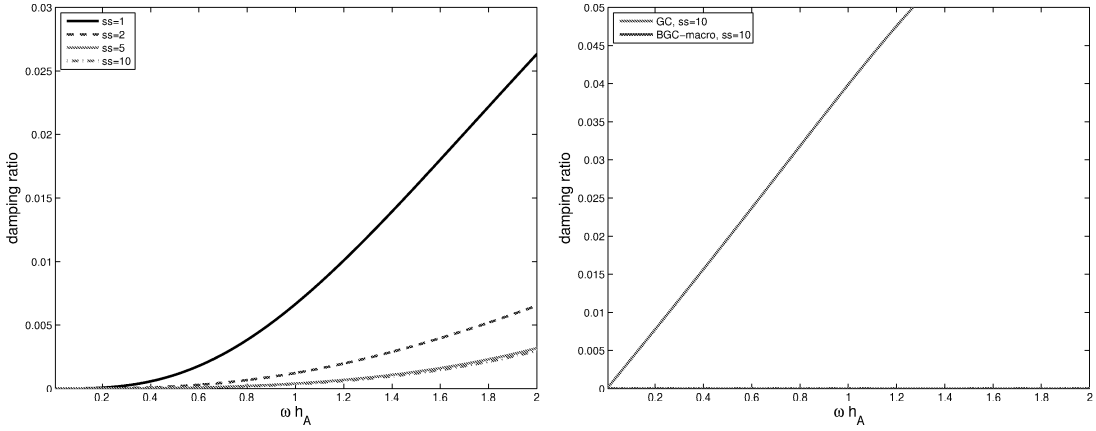

(a) BGC-macro method (α-schemes) (b) BGC-macro and GC methods (CAA schemes)

Figure 3: Numerical damping ratio $\bar{\xi}$ of the split oscillator ($b_1 = 1$): CH-α ($\rho_\infty = 0.8$) coupled with CH-α ($\rho_\infty = 0.5$) with different time step ratios ss. CAA coupled with CAA using BGC-macro and GC methods with $ss = 10$.

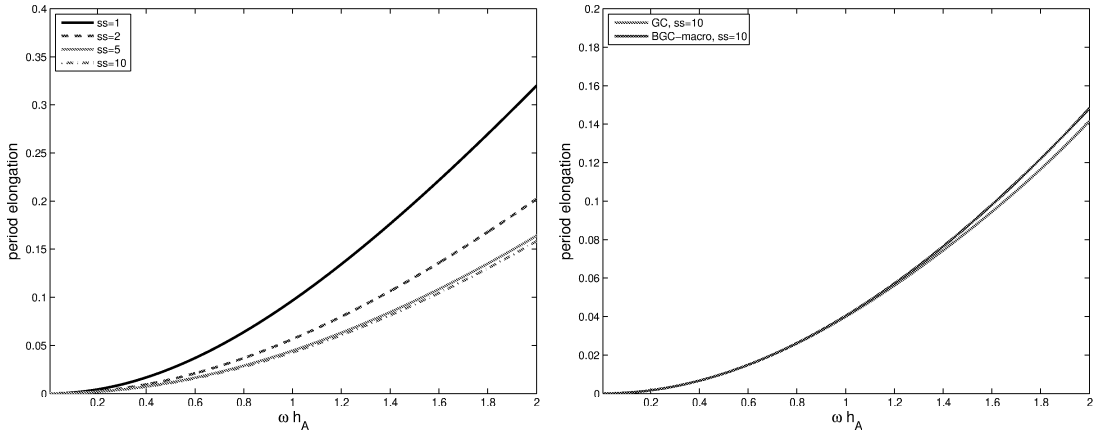

(a) BGC-macro method (α-schemes) (b) BGC-macro and GC methods (CAA schemes)

Figure 4: Period elongation $\frac{\bar{T}-T}{T}$ of the split oscillator ($b_1 = 1$): CH-α ($\rho_\infty = 0.8$) coupled with CH-α ($\rho_\infty = 0.5$) with different time step ratios ss. CAA coupled with CAA using BGC-macro and GC methods with $ss = 10$.

6 CONCLUSIONS

The paper presents a general methodology for building Heterogeneous Asynchronous Time Integrators based on energy considerations. It has been sought to cancel the interface pseudo-energy, originally introduced by Hughes in the energy method, for demonstrating the stability of hybrid time integration coupling methods related with homogeneous and heterogeneous time steps. The first method, called BGC-macro method, solves the interface problem, whose Lagrange multipliers at the interface are the unknowns, at the macro time scale by deriving from the zero value of the interface pseudo-energy a kinematic constraint at the interface expressed in terms of velocity increments. A linear assumption on the variation of the Lagrange multipliers over the macro time step is adopted. Then, the kinematic constraint at the macro time scale is modified so as to comply with a micro time scale approach. The second new coupling method, called BGC-micro method, is deduced from the previous macro-time based method, and is also able to couple Newmark and α-schemes.
From energy arguments, both methods are stable. It has been confirmed by the convergence analysis through the spectral analysis of the amplification matrix. In addition to the stability, the BGC-macro method is found to be second-order accurate when dealing with Newmark and α-schemes. The algorithmic damping ratio and the period elongation error are of the same order than the original properties of the α-schemes, despite the addition of Lagrange multipliers (the equations of motion related to the subdomains along with the kinematic constraint constituting a DAE). The BGC-micro method exhibits a first order accuracy when dealing with different time steps but is more versatile for a wide range of engineering dynamics problems, such as non linear dynamics, co-simulations, PsD tests and multiphysics applications (FSI). Developments are in progress to extend the BGC-micro approach at the same level of accuracy than the BGC-macro method.

References

Arnold, M., and O. Bruls, Convergence of the generalized-α scheme for constraint mechanical systems, *Multibody System Dynamics*, *18*, 185–202, 2007.

Bonelli, A., O. Bursi, L. He, G. Magonette, and P. Pegon, Convergence analysis of a parallel interfield method for heterogeneous simulations with dynamic substructuring, *International Journal for Numerical Methods in Engineering*, *75*, 800–825, 2008.

Bonnet, P., M. Williams, and A. Blakeborough, Evaluation of numerical time-integration schemes for real-time hybrid testing, *Earthquake Engineering and Structural Dynamics 2008*, *37*, 1467–1490, 2008.

Brun, M., A. Batti, A. Limam, and A. Combescure, Implicit/explicit multi-time step co-computations for predicting reinforced concrete structure response under earthquake loading, *Soil dynamics and Earthquake Engineering*, *33*, 19–37, 2012.

Brun, M., A. Batti, A. Combescure, and A. Gravouil, External coupling software based on macro- and micro-time scales for explicit/implicit multi-time-step co-computations in structural dynamics, *Finite Elements in Analysis & Design*, *52*, 41–59, 2014.

Brun, M., A. Gravouil, A. Combescure, and A. Limam, Two feti-based heterogeneous time step coupling methods for newmark and alpha-schemes derived from the energy method, *Computer Methods in Applied Mechanics and Engineering*, *283*, 130–176, 2015.

Bursi, O., L. He, A. Bonelli, and P. Pegon, Novel generalized-α methods for interfield parallel integration of heterogeneous structural dynamic systems, *Journal of Computational and Applied Mathematics*, *234*, 2250–2258, 2010.

Chung, J., and G. Hulbert, A time integration algorithm for structural dynamics with improved numerical dissipation: the generalized-α method, *Journal of Applied Mechanics*, *60*, 371–375, 1993.

Combescure, A., and A. Gravouil, A numerical scheme to couple subdomains with different time-steps for predominantly linear transient analysis, *Computer methods in applied mechanics and engineering*, *191*, 1129–1157, 2002.

Combescure, D., and P. Pegon, α-operator splitting time integration technique for pseudodynamic testing - error propagation analysis, *Soil Dynamics and Earthquake Engineering*, *16*, 427–443, 1997.

Geradin, M., and D. Rixen, *Theorie des Vibrations. Application la dynamique des structures.*, Masson, Paris,, 1993.

Gravouil, A., and A. Combescure, A multi-time-step explicit-implicit method for non-linear structural dynamics, *International Journal for Numerical Methods in Engineering*, *50*, 199–225, 2001.

Hilber, H., T. Hughes, and R. Taylor, Improved numerical dissipation for time integration algorithms in structural dynamics, *Earthquake Engineering and Structural Dynamics*, *5*, 283–292, 1977.

Hughes, T., *The Finite Element Method: Linear Static and Dynamic Finite Element Analysis*, Prentice-Hall, Englewood Cliffs, NJ, 1987.

Krenk, S., Extended state-space time intergation with high-frequency energy dissipation, *International Journal for Numerical Methods in Engineering*, *73*, 1767–1787, 2008.

Krenk, S., and J. Hogsberg, Properties of time intergation with first order filter damping, *International Journal for Numerical Methods in Engineering*, *64*, 547–566, 2005.

Mahjoubi, N., A. Gravouil, A. Combescure, and N. Greffet, A monolithic energy conserving method to couple heterogeneous time integrators with incompatible time steps in structural dynamics, *Computer methods in applied mechanics and engineering*, *200*, 1069–1086, 2011.

Masuri, S., A. Hoitink, X. Zhou, and K. Tamma, Algorithms by design: Part ii: A novel normalized time weighted residual methodology and design of a family of symplectic-momentum conserving algorithms for nonlinear structural dynamics, *International Journal for Computational Methods in Engineering Science and Mechanics*, *10*(1), 27–56, 2009a.

Masuri, S., A. Hoitink, X. Zhou, and K. Tamma, Algorithms by design: Part iii: A novel normalized time weighted residual methodology and design of optimal symplectic-momentum based controllable numerical dissipative algorithms for nonlinear structural dynamics, *International Journal for Computational Methods in Engineering Science and Mechanics*, *10*(1), 57–90, 2009b.

Masuri, S., A. Hoitink, X. Zhou, and K. Tamma, Algorithms by design: A new normalized time-weighted residual methodology and design of a family of energy-momentum conversing algorithms for non-linear structural dynamics, *International Journal for Numerical Methods in Engineering*, *79*, 1094–1146, 2009c.

Pinto, A., P. Pegon, G. Magonette, and G. Tsionis, Pseudo-dynamic testing of bridges using non-linear substructuring, *Earthquake Engineering and Structural Dynamics*, *33*, 1125–1146, 2004.

Prakash, A., and K. Hjelmstad, A feti-based multi-time-step coupling method for newmark schemes in structural dynamics, *International Journal for Numerical Methods in Engineering 2004*, *61*, 2183–2204, 2004.

Simo, J., and N. Tarnow, The discrete energy-momentum method: conserving algorithms for nonlinear elastodynamics, *Z. Angew. Math. Phys.*, *43*, 757–792, 1992.

Wood, W., M. Bossak, and O. Zienkiewicz, An alpha modification of newmark's method, *International Journal for Numerical Methods in Engineering*, *15*, 1562–1566, 1981.